



Multi-compound polarization by DNP allows simultaneous assessment of multiple enzymatic activities *in vivo*

David M. Wilson^a, Kayvan R. Keshari^{a,c}, Peder E.Z. Larson^a, Albert P. Chen^b, Simon Hu^a, Mark Van Criekinge^a, Robert Bok^a, Sarah J. Nelson^a, Jeffrey M. Macdonald^c, Daniel B. Vigneron^a, John Kurhanewicz^{a,*}

^a Department of Radiology, University of California San Francisco (UCSF), San Francisco, CA, United States

^b GE Healthcare, Menlo Park, CA 94025, United States

^c Department of Biomedical Engineering, University of North Carolina Chapel Hill (UNC-CH), Chapel Hill, NC, United States

ARTICLE INFO

Article history:

Received 24 November 2009

Revised 21 April 2010

Available online 27 April 2010

Keywords:

Hyperpolarized ¹³C
[1-¹³C]pyruvic acid
¹³C-sodium bicarbonate
[1,4-¹³C]fumaric acid
¹³C-urea
pH

ABSTRACT

Methods for the simultaneous polarization of multiple ¹³C-enriched metabolites were developed to probe several enzymatic pathways and other physiologic properties *in vivo*, using a single intravenous bolus. A new method for polarization of ¹³C sodium bicarbonate suitable for use in patients was developed, and the co-polarization of ¹³C sodium bicarbonate and [1-¹³C] pyruvate in the same sample was achieved, resulting in high solution-state polarizations (15.7% and 17.6%, respectively) and long spin–lattice relaxation times (T_1) (46.7 s and 47.7 s respectively at 3 T). Consistent with chemical shift anisotropy dominating the T_1 relaxation of carbonyls, T_1 values for ¹³C bicarbonate and [1-¹³C] pyruvate were even longer at 3 T (49.7 s and 67.3 s, respectively). Co-polarized ¹³C bicarbonate and [1-¹³C] pyruvate were injected into normal mice and a murine prostate tumor model at 3 T. Rapid equilibration of injected hyperpolarized ¹³C sodium bicarbonate with ¹³C CO₂ allowed calculation of pH on a voxel by voxel basis, and simultaneous assessment of pyruvate metabolism with cellular uptake and conversion of [1-¹³C] pyruvate to its metabolic products. Initial studies in a Transgenic Adenocarcinoma of Mouse Prostate (TRAMP) model demonstrated higher levels of hyperpolarized lactate and lower pH within tumor, relative to surrounding benign tissues and to the abdominal viscera of normal controls. There was no significant difference observed in the tumor lactate/pyruvate ratio obtained after the injection of co-polarized ¹³C bicarbonate and [1-¹³C] pyruvate or polarized [1-¹³C] pyruvate alone. The technique was extended to polarize four ¹³C labelled substrates potentially providing information on pH, metabolism, necrosis and perfusion, namely [1-¹³C]pyruvic acid, ¹³C sodium bicarbonate, [1,4-¹³C]fumaric acid, and ¹³C urea with high levels of solution polarization (17.5%, 10.3%, 15.6% and 11.6%, respectively) and spin–lattice relaxation values similar to those recorded for the individual metabolites. These studies demonstrated the feasibility of simultaneously measuring *in vivo* pH and tumor metabolism using nontoxic, endogenous species, and the potential to extend the multi-polarization approach to include up to four hyperpolarized probes providing multiple metabolic and physiologic measures in a single MR acquisition.

© 2010 Elsevier Inc. All rights reserved.

1. Introduction

A significant advantage of hyperpolarized MR metabolic imaging using dynamic nuclear polarization (DNP) is the ability to probe metabolic fluxes in real time, at high signal-to-noise [1]. *In vivo* hyperpolarized MR is unprecedented in its ability to characterize specific enzymatic pathways [2,3]. Most studies to date have focused on the last step of glycolysis in which [1-¹³C] pyruvate is

enzymatically converted to a number of products, including [1-¹³C] lactate mediated by the activity of lactate dehydrogenase (LDH) [3–7]. This pathway is associated with the Warburg effect, which postulates increased metabolism to lactate in tumor cells relative to normal tissue [8]. More recently, a number of additional pathways have been probed, for example the conversion of bicarbonate to CO₂ as mediated by carbonic anhydrase, and the conversion of glutamine to glutamate catalyzed by glutaminase [9,10]. Investigation of these processes by DNP–NMR has allowed mapping of pH *in vivo* and assessment of glutaminase activity in hepatic tumor cells. Additional agents showing promise in animals or perfused heart models include [2-¹³C] pyruvate, [2-¹³C] fructose, and [1-¹³C] lactate itself [11–13]. As the number of useful DNP

* Corresponding author. Address: Urology and Pharmaceutical Chemistry, Byers Hall, Room 203E, 1700 4th Street, San Francisco, CA 94158-2330, United States. Fax: +1 415 514 4714.

E-mail address: John.Kurhanewicz@radiology.ucsf.edu (J. Kurhanewicz).

agents continues to expand, the ability to probe multiple pathways and mechanisms simultaneously may provide valuable metabolic “signatures” associated with specific types of tumor and other diseased tissue. ^1H MRS is well established as a means to establish metabolic profiles in diseased tissue *in vivo* [14,15], but hyperpolarized MR has the additional capacity to provide kinetic information. A particular conversion pattern observed in diseased tissue may aid in targeting regions of pathology for biopsy or focal therapy, and/or better characterize the extent or aggressiveness of disease present prior to or after treatment. ^{13}C sodium bicarbonate has special promise due to its lack of toxicity and ability to probe physiological pH [9]. A broad number of pathologic processes demonstrate alterations in pH, including neoplastic, ischemic, and inflammatory conditions [16–19].

The dynamic nuclear polarization process requires the ^{13}C labelled probe compound to be in an amorphous (glassy) solid state with the appropriate free radical concentration at low temperatures ($\sim 1.2\text{ K}$) [1]. To accomplish an optimal preparation of a new probe or combinations of probes, the concentration of the desired agent(s), solvent/glassing agent(s), presence, concentration and type of a gadolinium agent, and the concentration and type of free radical must all be optimized. In addition, appropriate dissolution media must be prepared for each agent in order to ensure physiological pH, osmolarity, and to preserve the longest possible T_1 . In this manuscript, a method for polarization of ^{13}C sodium bicarbonate is reported, without requiring the removal of cesium as in the prior published method. This method has been combined with a co-polarization technique that allows simultaneous polarization of ^{13}C bicarbonate and $[1-^{13}\text{C}]$ pyruvate, to perform both pH and metabolic mapping *in vivo* using a single intravenous bolus. The technique was subsequently extended to polarize four ^{13}C labelled substrates, namely $[1-^{13}\text{C}]$ pyruvic acid, ^{13}C sodium bicarbonate, $[1,4-^{13}\text{C}]$ fumaric acid, and ^{13}C urea *in vitro* demonstrating the potential of obtaining information on pH, metabolism, necrosis and perfusion, in a single *in vivo* imaging experiment.

2. Materials and methods

2.1. Sample preparation

In all cases the ^{13}C compounds were purchased from Isotec (Miamisburg, OH) and used without further purification. All natural abundance chemicals and solvents were obtained from Aldrich (Miamisburg, OH). ^{13}C sodium bicarbonate: 135 mg of ^{13}C -sodium bicarbonate were dissolved in 1099 mg of glycerol, in a sealed flask while heating with a heat-gun. The hot solution was then passed through a 0.45 μm Millipore MCE Membrane filter (Fisher Scientific), and OX63 radical (Oxford Instruments, Abingdon, UK) was then dissolved to a final concentration of 20 mM. ^{13}C pyruvic acid: To a neat sample of $[1-^{13}\text{C}]$ pyruvic acid was added OX63 radical to a final concentration of 15 mM. ^{13}C fumaric acid: 350 mg of $[1,4-^{13}\text{C}]$ fumaric acid were mixed with 500 μL of dimethyl sulfoxide and OX63 was added to a final concentration of 15 mM. ^{13}C urea: 390 mg of ^{13}C -urea were dissolved in 895 mg of glycerol (Aldrich), and OX63 was added to a final concentration of 15 mM.

2.2. Co-polarization of ^{13}C -sodium bicarbonate with $[1-^{13}\text{C}]$ pyruvic acid

For studies at 11.7 T, 125 mg of the ^{13}C sodium bicarbonate preparation were placed in a sample cup and frozen in liquid nitrogen, followed by addition of 2.2 μL of pyruvic acid preparation. The sample was rapidly frozen to avoid mixing of the materials, and polarized at 94.074 GHz and 1.2–1.4 K for 3.5 h using a Hypersense DNP polarizer (Oxford Instruments, Abingdon, UK). This micro-

wave frequency corresponded to the optimum microwave frequency for the ^{13}C sodium bicarbonate sample, which was approximately 10 MHz lower than the optimum frequency observed for $[1-^{13}\text{C}]$ pyruvic acid. The solid-state polarization build-up curve was fit to the equation: $P(t) = P_{\text{eq}}(1 - \exp(-t/T_{\text{buildup}})) + \text{baseline}$, where P_{eq} is the equilibrium polarization achieved for the sample and T_{buildup} is the polarization build-up time constant. The resulting time constant was on the order of 3500 s, similar to that observed for the ^{13}C bicarbonate preparation alone. The sample was subsequently dissolved in 6.3 mL of water containing 0.3 mM EDTA. The solution was mixed manually in a teardrop flask, and injected using a 5 cc syringe into a previously shimmed 10 mm NMR tube at 37 °C. This process required approximately 15 s. Percentage polarizations were quantified in solution by measuring the signal enhancement obtained by DNP polarization compared to the signal at thermal equilibrium. For studies at 3 T, an identical polarization procedure was used except 250 mg of the sodium bicarbonate solution were used, combined with 4.5 μL of pyruvic acid and dissolved using 6.3 mL of water/EDTA.

2.3. Multi-compound polarization of ^{13}C sodium bicarbonate, pyruvic acid, urea and fumaric acid

For studies at 11.7 T, the following sample preparations (described above) were placed in a sample cup and frozen in liquid nitrogen: 30.0 μL sodium bicarbonate, 1.0 μL pyruvic acid, 6.0 μL urea 3.0 μL fumaric acid. The compounds were polarized at 94.080 GHz and 1.2–1.4 K for 2 h and subsequently dissolved in 5.0 mL of 100 mM phosphate buffer (pH = 7.8). Following dissolution, the sample was treated as above. In a separate set of experiments, identical quantities of these ^{13}C compounds were individually polarized by the usual method and dissolved using the same buffer. For murine studies at 3 T, an identical polarization procedure was used except 175 mg of the sodium bicarbonate solution were used, combined with 3 μL of pyruvic acid, 8 μL of fumaric acid and 20 μL of urea. Additionally, 8 μL of 10 M NaOH solution was frozen on top of the mixture. The sample was polarized as above and dissolved using 6.3 mL of water/EDTA.

2.4. Hyperpolarized ^{13}C spectroscopic studies

All 11.7 T NMR studies were performed on a 11.7 T Varian INOVA spectrometer (125 MHz ^{13}C , Varian Instruments) using a 10 mm $^{15}\text{N}/^{31}\text{P}/^{13}\text{C}$ triple-tuned direct detect probe. For the acquisition of hyperpolarized ^{13}C spectra of bicarbonate and pyruvate eighty proton-decoupled (WALTZ-16, 9000 Hz bandwidth, decoupling during acquisition only) pulse and acquire hyperpolarized ^{13}C NMR spectra (one average, spectral window = 4000 Hz, number of points = 16,000, TR = 3.0 s, acq time = 500 ms, total acq time = 300 s) were acquired every 3 s using a 5° pulse. Spin-lattice (T_1) relaxation times were determined by performing a mono-exponential fit to the signal decay curve of the hyperpolarized compounds. In all cases the r^2 value for the fit was >0.999 where r = the Pearson product moment correlation coefficient. All spectral measurements were collected at 37 °C. Signal enhancements due to hyperpolarization were calculated by integrating bicarbonate and pyruvate peaks in the first spectrum of the hyperpolarized dynamic experiment, and comparing these to the corresponding peaks in the thermal spectrum, accounting for differences in tip angle and the number of transients obtained.

2.5. 3 T T_1 measurements

All studies were performed using a 3 T GE Signa™ scanner (GE Healthcare, Waukesha, WI) equipped with the MNS (multinuclear spectroscopy) hardware package. The RF coil used was a

dual-tuned ^1H - ^{13}C coil used in prior hyperpolarized ^{13}C pyruvate mouse imaging studies [4,6]. For the T_1 measurement experiments, a half-echo FID sequence was used (5° non-selective RF excitation, spectral window of 5 kHz with 2048 points, TR = 3.0 s, 64 acquisitions, total acquisition time = 194 s). Magnitude spectra were used for data processing, and magnitude decay curves were obtained for pyruvate, pyruvate-hydrate, bicarbonate and CO_2 , from which the T_1 's were fit to a mono-exponential decay function.

2.6. Murine studies

Five mice were imaged: a B6SJL male wild-type mouse (normal), and four Transgenic Adenocarcinoma of Mouse Prostate (TRAMP) mice. The coil setup was the same as described above for the T_1 measurements. T_2 -weighted ^1H images were acquired in three planes using a fast spin-echo (FSE) sequence for anatomical reference. ^{13}C spectroscopic imaging was acquired immediately upon completion of a 15 s, 350 μL injection of the dissolved co-polarized ^{13}C bicarbonate and $[1-^{13}\text{C}]$ pyruvate (55 mM ^{13}C bicarbonate and 10 mM ^{13}C pyruvate) and hyperpolarized $[1-^{13}\text{C}]$ pyruvate alone (10 mM) within the same imaging exam. Injection of the co-polarized solution was initiated approximately 10 s following dissolution, making the total time between dissolution and initiation of ^{13}C spectroscopic imaging 25 s. For the hyperpolarized MR spectroscopic imaging studies, a double spin-echo pulse sequence with a small, variable flip-angle excitation pulse, adiabatic refocusing pulses, and a flyback echo-planar readout trajectory was used to acquire *in vivo* 3D ^{13}C MRSI [20]. These used a half-echo FID acquisition, 8×8 matrix size, TR = 230 ms, TE = 5 ms, 10 mm slice, 10×10 mm in-plane resolution for 1.0 cc voxels, and a spectral window of 5000 Hz with 1024 points (TRAMP). The k -space data was acquired concentrically, with a progressive RF flip angle scheme to utilize all available magnetization. This resulted in a total acquisition time of 15 s. A tube with 8 M ^{13}C urea inserted alongside the mouse was used for RF pulse calibration. This data was processed using 5 Hz exponential apodization and Fourier transformed using in-house software, as previously reported [6]. For comparison studies in the TRAMP model, voxels were designated predominantly tumor versus benign, and pH and lactate to pyruvate ratios were determined using the relative peak heights of magnitude spectra. Significance was determined using a two-tailed Student t -test with $p < 0.05$ considered statistically significant.

3. Results

3.1. Co-polarization of ^{13}C -sodium bicarbonate with $[1-^{13}\text{C}]$ pyruvic acid and T_1 measurements

A preparation method for ^{13}C sodium bicarbonate in glycerol was developed, allowing for reasonable ^{13}C sodium bicarbonate concentrations in the preparation [1.8 M \approx half that achieved previously for cesium bicarbonate [9]] and a high solution-state polarization ($12.7 \pm 1.9\%$). The final concentration of sodium bicarbonate is currently limited by the lower solubility of sodium bicarbonate relative to cesium bicarbonate in water and the maximum volume of the preparation that can be polarized in the Hypersense DNP polarizer. Multi-compound polarization of ^{13}C -sodium bicarbonate (1.8 M) in glycerol and neat $[1-^{13}\text{C}]$ pyruvic acid (14.2 M) was performed by freezing the ^{13}C preparations separately within the same sample cup, prior to placement in the polarizer. For both 11.7 T ($N = 3$) and 3 T experiments ($N = 3$), polarization of samples containing both ^{13}C sodium bicarbonate and ^{13}C pyruvate resulted in a build-up time constant of approximately 3500 s, with greater than 95% polarization of the sample achieved at 3.5 h. This polarization build-up time is longer than the polarization build-up time for

^{13}C pyruvate alone (build-up time constant ≈ 900 s) but is comparable to the polarization build-up time of ^{13}C sodium bicarbonate alone. Following dissolution using EDTA/ H_2O , the concentrations of ^{13}C bicarbonate and $[1-^{13}\text{C}]$ pyruvate were 28.4 mM and 5.2 mM, respectively, with an average pH of 7.8. The average solution-state polarization was $15.7 \pm 1.2\%$ for bicarbonate and $17.6 \pm 0.9\%$ for pyruvate, which was not significantly different from the polarization obtained for each compound alone (Table 1). Representative data are shown in Fig. 1, which demonstrate large signal enhancements, and mono-exponential decay for $[1-^{13}\text{C}]$ pyruvate (171 ppm), $[1-^{13}\text{C}]$ pyruvate hydrate (179 ppm), $[1-^{13}\text{C}]$ lactate (182 ppm), ^{13}C bicarbonate (161 ppm) and ^{13}C carbon dioxide (125 ppm), with no significant impurities noted in the hyperpolarized dynamic spectrum. The carbon dioxide resonance was ≈ 22 -fold smaller than the bicarbonate resonance. Calculated mean T_1 's at 11.7 T were 46.7 ± 0.6 s for bicarbonate, and 47.7 ± 1.1 s for pyruvate. At 3 T the mean T_1 values were significantly longer for pyruvate 67.3 ± 2.5 s than at 11.7 T. The bicarbonate T_1 was also longer (49.7 ± 2.9 s) at 3 T, but this difference was not significant. The measured T_1 of carbon dioxide at 11.7 T (44.7 ± 0.6 s) was not significantly less than that of sodium bicarbonate.

3.2. Murine co-polarization studies

Co-polarized ^{13}C bicarbonate and $[1-^{13}\text{C}]$ pyruvate were injected into one normal and four tumor-bearing TRAMP mice in order to determine whether images of pyruvate metabolism and pH could be simultaneously obtained and that the presence of the ^{13}C bicarbonate did not affect pyruvate metabolism. For animal studies, a larger sample containing both ^{13}C bicarbonate and $[1-^{13}\text{C}]$ pyruvate was used, corresponding to injected concentrations of 55 mM and 10 mM, respectively. As shown in Figs. 2 and 3, well resolved hyperpolarized ^{13}C resonances for the labelled carbonyls of $[1-^{13}\text{C}]$ pyruvate, $[1-^{13}\text{C}]$ pyruvate hydrate, $[1-^{13}\text{C}]$ lactate, ^{13}C bicarbonate and ^{13}C carbon dioxide could be observed in both normal mice (Fig. 2) and in tumor containing TRAMP mice (Fig. 3). The chemical shifts of these compounds were not different from those observed in solution studies. Despite the significantly higher concentration of ^{13}C bicarbonate injected, and in contrast to what was observed in solution (Fig. 1), the observed *in vivo* bicarbonate peak was lower than the pyruvate peak. The ^{13}C carbon dioxide peak observed was on average 22.4-fold lower than the ^{13}C bicarbonate peak.

As previously reported, integration of ^{13}C bicarbonate and ^{13}C CO_2 peaks, and application of the Henderson-Hasselbalch equation allowed calculation of pH on a voxel by voxel basis and the creation of a pH images [9], as well as the corresponding hyperpolarized lactate images. A representative data set acquired for a normal (wild-type) mouse is shown in Fig. 2, demonstrating low levels of hyperpolarized lactate (Lac/Pyr = 0.20–0.52) and pH values in the normal physiologic range (7.28–7.40). Regions of highest hyperpolarized lactate in the normal mouse were in the kidneys

Table 1

Spin-lattice relaxation values, and % polarization achieved for multi-compound polarization at 11.7 T. T_1 's and signal enhancements were similar to those observed when the individual compounds were polarized separately and dissolved in an identical 100 mM pH 7.8 phosphate buffer. Standard deviations are reported ($N = 3$).

| Compound | T_1 (s) multipol | T_1 (s) alone | % Polarization multipol | % Polarization alone |
|--------------------------------|-----------------------|--------------------|----------------------------|----------------------------|
| ^{13}C bicarbonate | 43.3 ± 1.2 | 48.7 ± 0.6 | 10.3 ± 1.8 | 12.7 ± 1.9 |
| $[1-^{13}\text{C}]$ pyruvate | 48.3 ± 1.5 | 48.3 ± 0.6 | 17.5 ± 3.4 | 17.4 ± 1.5 |
| $[1,1-^{13}\text{C}]$ fumarate | 29.0 ± 1.0 | 29.3 ± 0.6 | 15.6 ± 1.9 | 12.0 ± 0.7 |
| $[1-^{13}\text{C}]$ urea | 43.0 ± 1.0 | 44.0 ± 0.3 | 11.6 ± 2.5 | 12.4 ± 0.4 |

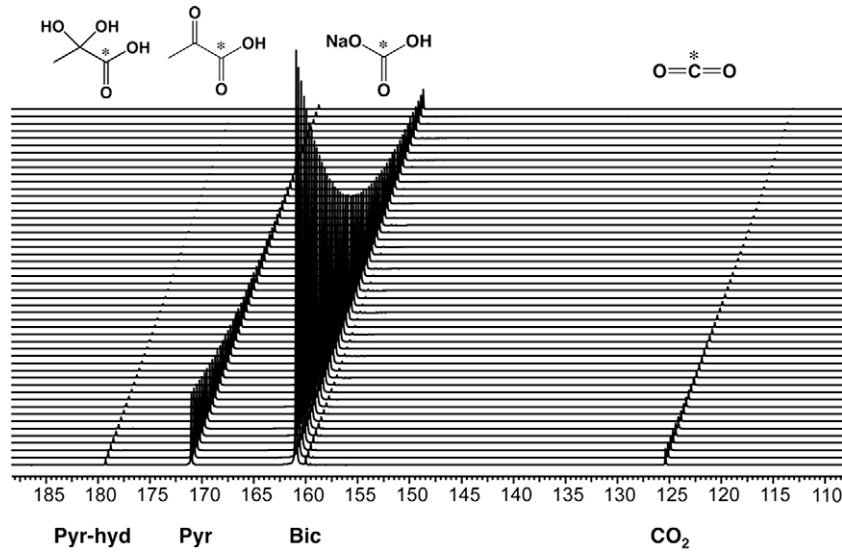


Fig. 1. Dynamic hyperpolarized spectrum for a co-polarized solution of [$1\text{-}^{13}\text{C}$] pyruvate and ^{13}C sodium bicarbonate, with data collected at 11.7 T. The final solution pH was 7.8–7.9. The mono-exponential decay for bicarbonate and pyruvate peaks were used to calculate the T_1 's.

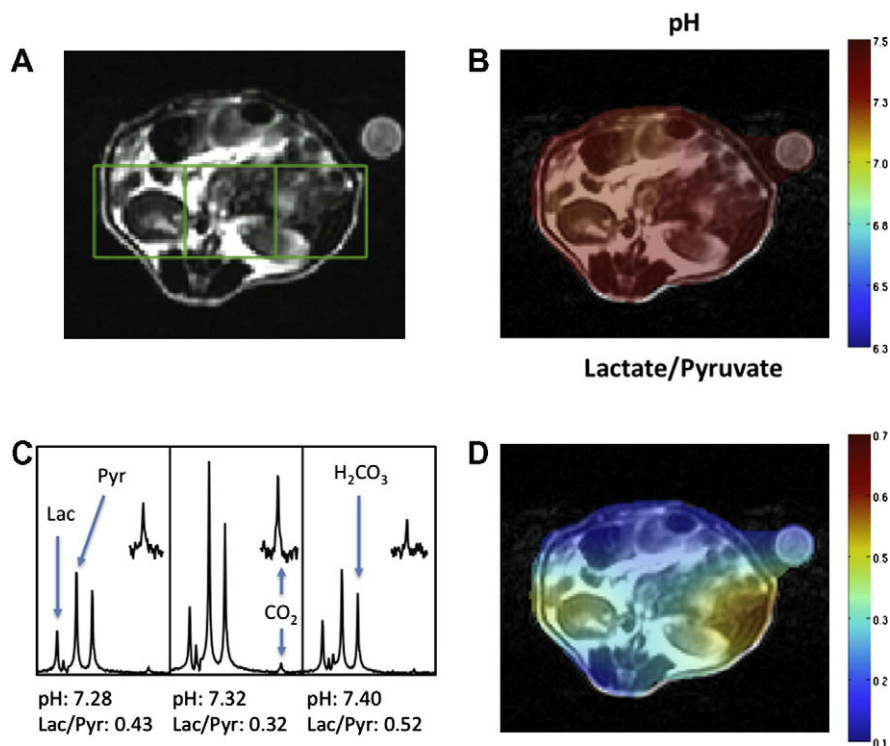


Fig. 2. *In vivo* data collected at 3 T. A T_2 weighted anatomic image (A), pH image of the same slice demonstrating the distribution of calculated pH (B), spectra for the corresponding voxels shown in the T_2 weighted image (C) and the lactate/pyruvate ratio image (D) are shown for a wild-type mouse. Following dissolution, 300 μL of a solution with 55 mM pre-polarized ^{13}C bicarbonate and 10 mM ^{13}C pyruvate were injected intravenously. Data were acquired with a resolution of 1 cm^3 . The pH for individual voxels was calculated using the Henderson–Hasselbalch equation and pK_a of 6.17 at 37 $^\circ\text{C}$. The peak ratios of observed ^{13}C lactate to ^{13}C pyruvate are shown beneath the corresponding spectra. Regions of the CO_2 resonance have been scaled up to demonstrate the signal-to-noise achieved in each voxel.

due to excretion of lactate, with most of the tissues in the normal mouse abdomen demonstrating Lac/Pyru ratios in the 0.2–0.3 range. Initial studies in TRAMP animals demonstrated higher levels of hyperpolarized lactate and more acidic pH values within tumor. A representative study is depicted in Fig. 3, showing higher levels of lactate (Lac/Pyru = 0.43–0.58) and more acidic pH (6.6–7.0) in the region of the prostate tumor as compared to surrounding benign abdominal tissues. The ability to distinguish tumor from sur-

rounding benign tissue was addressed by comparing voxels containing tumor ($N=5$) to those containing benign tissue ($N=5$). The average pH for the tumoral voxels (6.80 ± 0.15) was lower than that observed for those containing benign tissue (7.02 ± 0.18), although the results were not statistically significant ($P=0.11$). The average Lac/Pyru ratio observed for tumoral voxels (0.53 ± 0.19) was slightly higher than the ratio seen in benign tissues (0.44 ± 0.08), although not significantly ($P=0.60$). Evaluation

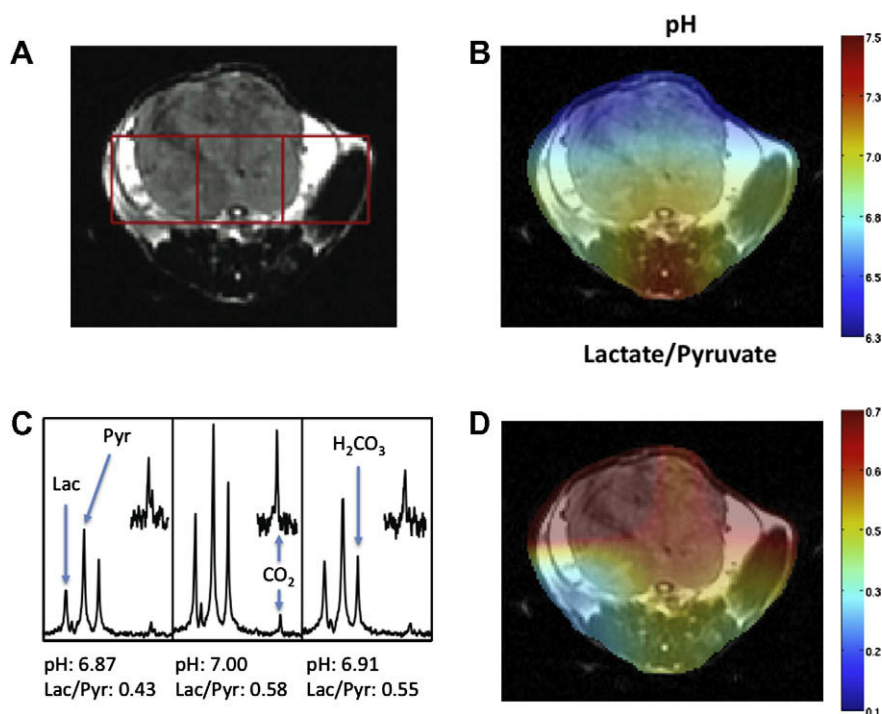


Fig. 3. *In vivo* data collected at 3 T. A T_2 weighted anatomic image (A), pH image of the same slice demonstrating the distribution of pH calculated (B), spectra for the corresponding voxels shown in the T_2 weighted image (C) and the lactate/pyruvate ratio image (D) are shown for a TRAMP tumor bearing mouse. The tumor is visible in the upper half of the slice. Following dissolution, 300 μL of a solution 55 mM in pre-polarized ^{13}C bicarbonate and 10 mM in ^{13}C pyruvate were injected intravenously. Data was acquired with a resolution of 1 cm^3 . The pH for individual voxels was calculated using the Henderson–Hasselbalch equation and pK_a of 6.17 at 37°C . The peak ratios of observed ^{13}C lactate to ^{13}C pyruvate are also shown beneath the corresponding spectra. Regions of the CO_2 resonance have been scaled up to demonstrate the signal-to-noise achieved in each voxel.

was limited by the difficulty in choosing voxels that were predominantly benign versus predominantly malignant, given the coarse spatial resolution of the studies. An additional set of experiments was performed in order to address the impact of ^{13}C bicarbonate co-administration on $[1-^{13}\text{C}]$ pyruvic acid metabolism *in vivo*. Pyruvate metabolism was not significantly different ($P = 0.4$) in TRAMP mice ($N = 4$) that were injected with hyperpolarized $[1-^{13}\text{C}]$ pyruvate alone (mean tumor lactate to pyruvate ratio (Lac/Pyr) = 0.47 ± 0.18) and in combination with hyperpolarized ^{13}C bicarbonate (mean tumor Lac/Pyr = 0.41 ± 0.18) within the same study.

3.3. Multi-compound polarization

In order to demonstrate that more than two compounds could be polarized in the same sample without significant loss of T_1 or enhancement, four substrates of metabolic and physiologic interest were polarized: $[1-^{13}\text{C}]$ pyruvic acid, ^{13}C sodium bicarbonate, $[1,1-^{13}\text{C}]$ fumaric acid, and $[1-^{13}\text{C}]$ urea. Again, these compounds were frozen separately in a Hypersense polarizer sample cup and polarized at a microwave frequency of 94.080 GHz. Since not every compound could be polarized at its ideal frequency, a compromise value was chosen to provide the best simultaneous polarization of the mixture. The multi-polarization had a build-up time constant of approximately 3500 s, with greater than 95% polarization of the sample achieved at 3.5 h identical to the co-polarization, indicating the polarization time was dominated by the slower polarization of ^{13}C sodium bicarbonate. On dissolution using EDTA/ H_2O , the concentrations of ^{13}C bicarbonate, $[1-^{13}\text{C}]$ pyruvate, $[1,1-^{13}\text{C}]$ fumaric acid, and $[1-^{13}\text{C}]$ urea were 10.8 mM, 2.8 mM, 2.5 mM and 7.8 mM respectively, with a measured pH of 7.8–7.9. A representative resulting hyperpolarized spectrum ($t = 60\text{ s}$) is presented in Fig. 4a, with calculated T_1 's, and enhancements presented in Ta-

ble 1. Fig. 4 demonstrates well-resolved resonances for all of the ^{13}C labelled carbonyls; $[1-^{13}\text{C}]$ pyruvate (171 ppm), $[1-^{13}\text{C}]$ pyruvate hydrate (179 ppm), ^{13}C bicarbonate (161 ppm) and ^{13}C carbon dioxide (125 ppm), urea (164 ppm) and fumarate (175 ppm) with one unknown small impurity at 160 ppm. In a second set of experiments, the compounds were polarized separately under identical conditions, and dissolved in a high buffering-capacity buffer to ensure a similar pH (7.8) to that observed for the multi-metabolite case. In all cases the calculated T_1 's and enhancements were similar, demonstrating that multi-compound polarization can be achieved with minimal if any loss of SNR (Table 1). For *in vivo* applications, the polarization protocol was modified slightly in order to allow higher concentrations of the hyperpolarized ^{13}C agents, and minimize loss of solution-state polarization following dissolution. Representative data are shown in Fig. 4b demonstrating resolution of all four metabolites *in vivo* at high SNR, albeit with relatively coarse spatial resolution (1 cm^3).

4. Discussion

Multi-metabolite polarization is intended to circumvent one of the main drawbacks of DNP, namely its long polarization times, by polarizing several precursors at the same time, and then developing a biological scenario whereby the inevitably very complex metabolic data *in vivo* can be analyzed. In this study, a method for direct polarization of ^{13}C sodium bicarbonate suitable for use in patients was developed, and the co-polarization of ^{13}C sodium bicarbonate and $[1-^{13}\text{C}]$ pyruvate in a single intravenous bolus was achieved for the first time. The polarization build-up time was longer than the polarization build-up time for $[1-^{13}\text{C}]$ pyruvate alone (build-up time constant $\approx 900\text{ s}$) due to the longer polarization build-up time of ^{13}C sodium bicarbonate. However, the use of

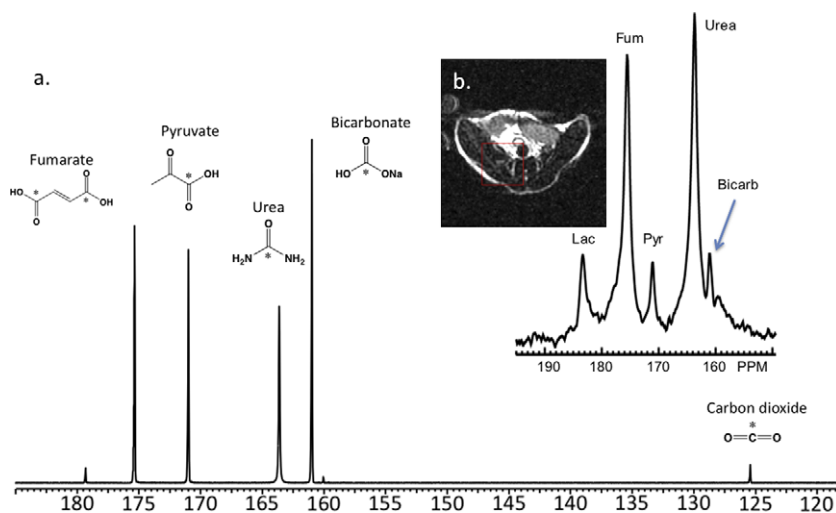


Fig. 4. (a) Multi-compound polarization of four ^{13}C biomolecules of interest: fumarate, pyruvate, urea, and bicarbonate *in vitro*. These data were obtained in a 10 mm NMR tube 60 s following dissolution at 11.7 T. Levels of polarization achieved were similar to that obtained for the individual compounds, performed using an optimized microwave frequency. T_1 's in solution were similar to those obtained for the separate species. Standard deviations are reported ($N = 3$). (b) Multi-compound polarization *in vivo* performed in a TRAMP mouse model at 3 T.

gadolinium contrast agent in the preparation can significantly increase the polarization of the compound ($19.3 \pm 1.4\%$ in initial studies, $N = 3$), which can either increase the overall signal or decrease the build-up time to achieve the same signal. The ^{13}C sodium bicarbonate preparation provided hyperpolarized bicarbonate concentrations that were approximately half (55 mM) that previously reported for cesium bicarbonate (100 mM), and similar solution-state polarizations ($\approx 16\%$) without the need for chromatography following dissolution to remove the cesium [9]. Consistent with chemical shift anisotropy dominating the T_1 relaxation of carbonyls, the T_1 's of ^{13}C bicarbonate and $[1-^{13}\text{C}]$ pyruvate were even longer at 3 T (49.7 s and 67.3 s, respectively) as compared to 11.7 T [21,22]. As predicted by the Henderson–Hasselbalch equation ($\text{pH} = \text{pK}_a + \log_{10}([\text{HCO}_3^-]/[\text{CO}_2])$, $\text{pK}_a = 6.17$) [9] and the known pH and temperature of the solution, the carbon dioxide resonance was ≈ 22 -fold less than the bicarbonate resonance. However, the co-polarization resulted in sufficiently high solution-state polarizations and spin-lattice relaxation times of bicarbonate, carbon dioxide and pyruvate to acquire simultaneous *in vivo* images of interstitial pH and pyruvate metabolism in normal and tumor-bearing mice.

Despite the significantly higher concentration of ^{13}C bicarbonate than $[1-^{13}\text{C}]$ pyruvate injected in animal *in vivo* studies, and in contrast to what was observed in solution, the observed *in vivo* bicarbonate peak was much lower than the pyruvate peak. This reduction in hyperpolarized signal may be the result of ^{13}C carbon dioxide loss during the dissolution process, the much shorter *in vivo* T_1 of ^{13}C bicarbonate and carbon dioxide [9], as well as loss of ^{13}C carbon dioxide in the lungs with ventilation. The *in vivo* T_1 of ^{13}C bicarbonate and carbon dioxide has been previously reported to be ≈ 10 s, much shorter than the ≈ 50 s reported in the solution studies described herein. Most important for *in vivo* measurements of pH is the fact that the T_1 of ^{13}C bicarbonate and carbon dioxide are similar as reported in the solution state in this paper and *in vivo* previously [9]. The equivalence of the T_1 's is most likely due to the rapid inter-conversion of ^{13}C bicarbonate and carbon dioxide, since even in the absence of carbonic anhydrase the exchange is rapid ($\approx 0.1 \text{ s}^{-1}$) and accelerated by the enzyme [9]. Moreover, sufficient S/N data were obtained for magnetic resonance spectroscopic imaging studies with a 1 cm^3 spatial resolution. This relatively coarse spatial resolution was mandated by the roughly 20-fold difference in ^{13}C CO_2 peak signal-to-noise relative to the ^{13}C bicarbonate peak for pH's in the

physiologic range. However, this limitation in sensitivity can be overcome by increasing the amount of hyperpolarized ^{13}C bicarbonate infused. In the current study, the bicarbonate preparation in glycerol was 1.8 M, limiting the concentration of injected bicarbonate to 55 mM using existing methods on the Oxford HyperSense polarizer. When this method is applied to patient studies, the ^{13}C bicarbonate concentration will not be a problem since clinical DNP polarizers will have the ability to polarize and dissolve larger amounts of ^{13}C bicarbonate than the current HyperSense DNP polarizer. Bicarbonate is often infused into patients at high concentrations on the order of 150 mM.

Similar to what has been previously reported for the injection of hyperpolarized $[1-^{13}\text{C}]$ pyruvate alone in the normal and TRAMP mouse, higher levels of hyperpolarized $[1-^{13}\text{C}]$ lactate were observed in the TRAMP tumor compared to benign tissues in the abdomen of the mouse after injection of co-polarized ^{13}C bicarbonate and $[1-^{13}\text{C}]$ pyruvate [6]. However, given the limited sample size and relatively coarse spatial resolution achieved, more studies are clearly needed to validate changes in pH and $[1-^{13}\text{C}]$ pyruvate metabolism in the TRAMP model, interrogated via this method. Importantly, the presence of bicarbonate did not change the observed pyruvate metabolism with the same tumor hyperpolarized lactate/pyruvate ratios being obtained when pyruvate was administered alone or in combination with bicarbonate. Rapid equilibration of injected hyperpolarized ^{13}C sodium bicarbonate with ^{13}C CO_2 after injection in mice also allowed the calculation of pH on a voxel by voxel basis as previously described in a study of hyperpolarized ^{13}C cesium bicarbonate in a murine lymphoma model [9]. Our initial TRAMP studies demonstrated a tumoral pH similar to what has been previously reported for the pH of the EL4 tumor ($\text{pH} = 6.71 \pm 0.14$) [9]. These initial data suggested that the more acidic pH observed in cancerous tissue correlated with increased pyruvate to lactate conversion, supporting the hypothesis that the cellular evolution associated with carcinogenesis selects for lactate production resulting in microenvironmental acidosis. It has been proposed that this microenvironmental acidosis enables the malignant cells to breakdown and invade neighbouring tissue [23,24]. However, additional studies need to be performed in order to verify the correlation between hyperpolarized lactate production and decreased interstitial pH, and determine whether decreased tumor pH correlates with increasing pathologic grade as previously shown for hyperpolarized lactate production [6].

The co-polarization technique was extended to polarize four ^{13}C labelled substrates, namely $[1-^{13}\text{C}]$ pyruvic acid, ^{13}C sodium bicarbonate, $[1,4-^{13}\text{C}]$ fumaric acid, and ^{13}C urea, *in vitro* demonstrating the potential of obtaining information on pH, metabolism, necrosis and perfusion, with high levels of solution-state polarization (10–20%) and spin–lattice relaxation values (30–50 s) similar to those obtained with polarization of the individual hyperpolarized probes. In addition, initial studies demonstrated that these four ^{13}C probes could be simultaneously detected *in vivo*, at high SNR. Several challenges were encountered with respect to polarization and dissolution of these four probes. First, as discussed previously the Oxford Hypersense polarizer is limited in its ability to dissolve large volumes of ^{13}C sample preparations. Second, differences in ideal microwave irradiation frequencies for the four compounds resulted in several ^{13}C compounds being polarized off-resonance, limiting their solid-state polarization. Finally, fast chemical interactions (specifically acid-base) between polarized ^{13}C species in solution is likely limiting their solution-state polarization, and may in some cases affect T_1 . For example, when polarizing organic acids (such as fumaric acid and pyruvic acid) with sodium bicarbonate, a significant titration occurs during dissolution, with rapid generation of carbonic acid (and therefore CO_2), which reduces the hyperpolarized ^{13}C bicarbonate signal obtained both *in vitro* and *in vivo*. For the multi-metabolite studies, the detection of ^{13}C CO_2 was again limiting, and reliable pH values were not obtained. Future efforts will focus on augmenting the CO_2 resonance for high-resolution multi-metabolite studies employing these four compounds. ^{13}C urea has already been employed as an intravascular angiographic agent, and could be used in the described agent combination to assess tissue perfusion [1,7]. $[1,4-^{13}\text{C}]$ fumarate represents a point of entry into the citric acid cycle and has recently been shown to be a marker of treatment response through increased production of hyperpolarized $[1,4-^{13}\text{C}]$ malate due to increased cellular necrosis after therapy [25]. The labelled carbons of $[1,4-^{13}\text{C}]$ fumarate are magnetically equivalent (175 ppm), while the $[1,4-^{13}\text{C}]$ malate carbons are not equivalent ($[1-^{13}\text{C}]$ 181.8 ppm, $[4-^{13}\text{C}]$ 180.6 ppm). In a multi-polarization experiment, the $[1-^{13}\text{C}]$ resonance of malate can therefore overlap the $[1-^{13}\text{C}]$ resonance of lactate (182 ppm). Since the magnitude of the $[1-^{13}\text{C}]$ and $[4-^{13}\text{C}]$ resonances of malate are equal and the $[4-^{13}\text{C}]$ resonances does not overlap other resonances, it can be used to separate malate from lactate. For *in vivo* applications that have limited spectral resolution, deconvolution may be necessary to discern relative intensities of lactate and malate.

Simultaneous evaluation of enzymatic pathways and other physiologic properties is not easily achieved using other imaging methods including PET, optical imaging, or other targeted MR methods. As additional new ^{13}C agents are developed, multi-compound polarization will be a powerful method of probing multiple metabolic pathways and other physiologic properties simultaneously, in a single MR scan lasting only seconds.

Acknowledgments

We would like to acknowledge funding from the National Institutes of Health (R21 EB005363, R01 EB007588); NIBIB T32 Training Grant 1 T32 ED001631 as well as support from GE Healthcare. Grant sponsors: National Institutes of Health (R21 EB005363, R01 EB007588); NIBIB T32 Training Grant 1 T32 ED001631.

References

- [1] J.H. Ardenkjaer-Larsen et al., Increase in signal-to-noise ratio of >10,000 times in liquid-state NMR, *Proc. Natl. Acad. Sci. USA* 100 (18) (2003) 10158–10163.
- [2] K. Golman, J.H. Ardenkjaer-Larsen, J.S. Petersson, S. Mansson, I. Leunbach, Molecular imaging with endogenous substances, *Proc. Natl. Acad. Sci. USA* 100 (18) (2003) 10435–10439.
- [3] K. Golman, R.I. Zandt, M. Lerche, R. Pehrson, J.H. Ardenkjaer-Larsen, Metabolic imaging by hyperpolarized ^{13}C magnetic resonance imaging for *in vivo* tumor diagnosis, *Cancer Res.* 66 (22) (2006) 10855–10860.
- [4] S.J. Kohler et al., *In vivo* ^{13}C carbon metabolic imaging at 3 T with hyperpolarized ^{13}C -1-pyruvate, *Magn. Reson. Med.* 58 (1) (2007) 65–69.
- [5] M.E. Merritt et al., Hyperpolarized ^{13}C allows a direct measure of flux through a single enzyme-catalyzed step by NMR (Translated from English), *Proc. Natl. Acad. Sci. USA* 104 (50) (2007) 19773–19777 (in English).
- [6] M.J. Albers et al., Hyperpolarized ^{13}C lactate, pyruvate, and alanine: noninvasive biomarkers for prostate cancer detection and grading (Translated from English), *Cancer Res.* 68 (20) (2008) 8607–8615 (in English).
- [7] K. Golman et al., Molecular imaging using hyperpolarized ^{13}C (Translated from English), *Br. J. Radiol.* 76 (Spec No 2) (2003) S118–127 (in English).
- [8] O. Warburg, Origin of cancer cells (Translated from Ger), *Oncologia* 9 (2) (1956) 75–83 (in Ger).
- [9] F.A. Gallagher et al., Magnetic resonance imaging of pH *in vivo* using hyperpolarized ^{13}C -labelled bicarbonate (Translated from English), *Nature* 453 (7197) (2008) 940–943 (in English).
- [10] F.A. Gallagher, M.I. Kettunen, S.E. Day, M. Lerche, K.M. Brindle, ^{13}C MR spectroscopy measurements of glutaminase activity in human hepatocellular carcinoma cells using hyperpolarized ^{13}C -labeled glutamine (Translated from English), *Magn. Reson. Med.* 60 (2) (2008) 253–257 (in English).
- [11] M.A. Schroeder et al., Real-time assessment of Krebs cycle metabolism using hyperpolarized ^{13}C magnetic resonance spectroscopy (Translated from English), *FASEB J.* (2009) (in English).
- [12] A.P. Chen et al., Feasibility of using hyperpolarized $[1-^{13}\text{C}]$ lactate as a substrate for *in vivo* metabolic ^{13}C MRSI studies (Translated from English), *Magn. Reson. Imaging* 26 (6) (2008) 721–726 (in English).
- [13] K.R. Keshari et al., Hyperpolarized $[2-^{13}\text{C}]$ -fructose: a hemiketal DNP substrate for *in vivo* metabolic imaging (Translated from English), *J. Am. Chem. Soc.* 131 (48) (2009) 17591–17596 (in English).
- [14] W.P. Dillon, S. Nelson, What is the role of MR spectroscopy in the evaluation and treatment of brain neoplasms? (Translated from English), *AJNR Am J. Neuroradiol.* 20 (1) (1999) 2–3 (in English).
- [15] J. Kurhanewicz, M.G. Swanson, S.J. Nelson, D.B. Vigneron, Combined magnetic resonance imaging and spectroscopic imaging approach to molecular imaging of prostate cancer (Translated from English), *J. Magn. Reson. Imaging* 16 (4) (2002) 451–463 (in English).
- [16] M. Hohn-Berlage, Y. Okada, O. Kloiber, K.A. Hossmann, Imaging of brain tissue pH and metabolites. A new approach for the validation of volume-selective NMR spectroscopy (Translated from English), *NMR Biomed.* 2 (5–6) (1989) 240–245 (in English).
- [17] A. Syrota et al., Tomographic mapping of brain intracellular pH and extracellular water space in stroke patients (Translated from English), *J. Cereb. Blood Flow Metab.* 5 (3) (1985) 358–368 (in English).
- [18] M. Schindler, S. Grabski, E. Hoff, S.M. Simon, Defective pH regulation of acidic compartments in human breast cancer cells (MCF-7) is normalized in adriamycin-resistant cells (MCF-7adr) (Translated from English), *Biochemistry* 35 (9) (1996) 2811–2817 (in English).
- [19] M.R. Ciriolo et al., Loss of GSH, oxidative stress, and decrease of intracellular pH as sequential steps in viral infection (Translated from English), *J. Biol. Chem.* 272 (5) (1997) 2700–2708 (in English).
- [20] C.H. Cunningham et al., Double spin-echo sequence for rapid spectroscopic imaging of hyperpolarized ^{13}C (Translated from English), *J. Magn. Reson.* 187 (2) (2007) 357–362 (in English).
- [21] F.A.L. Anet, D.J. O'Leary, The Shielding Tensor, *Concepts Magn. Reson.* 4 (1992) 35–52.
- [22] J.S. Blicharski, Nuclear magnetic relaxation by anisotropy of the chemical shift, *Z. Naturforsch. A* (27) (1972) 1456–1458.
- [23] R.A. Gatenby, R.J. Gillies, Why do cancers have high aerobic glycolysis?, *Nat. Rev. Cancer* 4 (11) (2004) 891–899.
- [24] R.A. Gatenby, E.T. Gawlinski, A.F. Gmitro, B. Kaylor, R.J. Gillies, Acid-mediated tumor invasion: a multidisciplinary study, *Cancer Res.* 66 (10) (2006) 5216–5223.
- [25] F.A. Gallagher et al., Production of hyperpolarized $[1,4-^{13}\text{C}]$ malate from $[1,4-^{13}\text{C}]$ fumarate is a marker of cell necrosis and treatment response in tumors (Translated from English), *Proc. Natl. Acad. Sci. USA* 106 (47) (2009) 19801–19806 (in English).